SMART-Signal Phase II: Arterial Offset Optimization Using Archived High-Resolution Traffic Signal Data

Final Report

Prepared by:

Henry X. Liu
Heng Hu

Department of Civil Engineering
University of Minnesota

CTS 13-19

Technical Report Documentation Page

1. Report No.	2.	3. Recipients Accession No.	
CTS 13-19			
4. Title and Subtitle SMART-Signal Phase II: Arterial Offset Optimization Using Archived High-Resolution Traffic Signal Data		5. Report Date April 2013 6.	
7. Author(s) Henry X. Liu and Heng Hu		8. Performing Organization Report No.	
9. Performing Organization Name and Address Department of Civil Engineering University of Minnesota 500 Pillsbury Drive Minneapolis, MN 55455		10. Project/Task/Work Unit No. CTS Project #2009001 11. Contract (C) or Grant (G) No.	
12. Sponsoring Organization Name and Address Intelligent Transportation Systems Institute Center for Transportation Studies University of Minnesota 200 Transportation and Safety Building 511 Washington Ave. SE Minneapolis, MN 55455		13. Type of Report and Period Covered Final Report 14. Sponsoring Agency Code	
15. Supplementary Notes http://www.its.umn.edu/Publications/ResearchReports/			

16. Abstract (Limit: 250 words)

Traditionally, offset optimization for coordinated traffic signals is based on average travel times between intersections and average traffic volumes at each intersection, without consideration of the stochastic nature of field traffic. Using the archived high-resolution traffic signal data, in this project, we developed a data-driven arterial offset optimization model that will address two well-known problems with vehicle-actuated signal coordination: the early return to green problem and the uncertain intersection queue length problem. To account for the early return to green problem, we introduce the concept of conditional distribution of the green start times for the coordinated phase. To handle the uncertainty of intersection queue length, we adopt a scenario-based approach that generates optimization results using a series of traffic-demand scenarios as the input to the offset optimization model. Both the conditional distributions of the green start times and traffic demand scenarios can be obtained from the archived high-resolution traffic signal data. Under different traffic conditions, queues formed by side-street and main-street traffic are explicitly considered in the derivation of intersection delay. The objective of this model is to minimize total delay for the main coordinated direction and at the same time it considers the performance of the opposite direction. Due to model complexity, a genetic algorithm is adopted to obtain the optimal solution. We test the performance of the optimized offsets not only in a simulated environment but also in the field. Results from both experiments show that the proposed model can reduce travel delay of coordinated direction significantly without compromising the performance of the opposite approach.

17. Document Analysis/Descriptors	18. Availability Statement		
Traffic signals, Offsets (Traffic signal timing), Optimization, Genetic algorithms, Archived high-resolution traffic signal data	No restrictions. Document available from: National Technical Information Services, Alexandria, Virginia 22312		
19. Security Class (this report) Unclassified	20. Security Class (this page) Unclassified	21. No. of Pages 37	22. Price

SMART-Signal Phase II: Arterial Offset Optimization Using Archived High-Resolution Traffic Signal Data

Final Report

Prepared by:

Henry X. Liu
Heng Hu

Department of Civil Engineering
University of Minnesota

April 2013

Published by:

Intelligent Transportation Systems Institute
Center for Transportation Studies
University of Minnesota
200 Transportation and Safety Building
511 Washington Avenue SE
Minneapolis, Minnesota 55455

Acknowledgments

The authors wish to acknowledge those who made this research possible. The study was funded by the Intelligent Transportation Systems (ITS) Institute, a program of the University of Minnesota's Center for Transportation Studies (CTS). Additional financial support was provided by the United States Department of Transportation Research and Innovative Technologies Administration (RITA). The authors also would like to thank Mr. Steve Misgen and his staff from the Minnesota Department of Transportation for their support on the field implementation of the SMART (Systematic Monitoring of Arterial Road Traffic)-Signal system.

Dr. Henry Liu and the University of Minnesota have equity and royalty interests in SMART-Signal Technologies, Inc., a Minnesota-based private company which may commercially benefit from the results of this research. These relationships have been reviewed and managed by the University of Minnesota in accordance with its Conflicts of Interests policies.

Table of Contents

List of Figures

List of Tables

Executive Summary

Traditionally, offset optimization for coordinated traffic signals is based on average travel times between intersections and average traffic volumes at each intersection, without consideration of the stochastic nature of field traffic. Using the high-resolution traffic signal data collected by the SMART (Systematic Monitoring of Arterial Road Traffic)-Signal system, in this project, we developed a data-driven arterial offset optimization model.

The proposed model addresses two well-known problems with vehicle-actuated signal coordination: the early return to green problem and the uncertain intersection queue length problem. To account for the early return to green problem, we introduce the concept of conditional distribution of the green start times for the coordinated phase. To handle the uncertainty of intersection queue length, we adopt a scenario-based approach that generates optimization results using a series of traffic demand scenarios as the input to the offset optimization model. Both the conditional distributions of the green start times and traffic-demand scenarios can be obtained from the archived high-resolution traffic signal data. Under different traffic conditions, queues formed by side-street and main-street traffic are explicitly considered in the derivation of intersection delay. The objective of this offset optimization model is to minimize total delay for the main coordinated direction and at the same time it considers the performance of the opposite direction. Due to the model complexity, a genetic algorithm is adopted to obtain the optimal solution.

We took six intersections along the TH55 in Minneapolis, MN as the study site and this corridor has a total length of 1.83 miles with a speed limit of 55 MPH. Ten weekdays' high-resolution traffic signal data during the morning peak hours from 6/15/2009 to 6/26/2009 was utilized to generate the optimal offsets. We implemented the optimized offset values in both VISSIM simulation model and the field signal controllers. Both test results indicate that the model can reduce travel delay of coordinated direction significantly without compromising the performance of the opposite approach. In practice, we envision that our optimization program can be utilized periodically (for example, every few weeks) to optimize system performance using the archived data during that period.

Chapter 1. Introduction

Offset settings are critical to the performance of traffic signal system operated in a coordinated mode. Over the years many computerized programs have been developed for signal offset optimization, using average traffic volume at intersections and average travel times between intersections. Based on the objectives of the optimization process, these programs can be divided into two groups. One group aims to maximize the bandwidth and progression along arterials, such as MAXBAND (Little et al., 1981) and PASSER II (TTI, 2009), and the other group attempts to minimize system delay and number of stops, such as TRANSYT-7F(Wallace et al., 1984) and Synchro (Trafficware, 2001). In more detail, MAXBAND maximizes weighted combination of bandwidths given cycle length and splits. It allows users to input a queue clearance time for each approach, but the queuing process is not considered inside the model. PASSER II maximizes the bandwidth efficiency based on pre-calculated splits. Traffic performance measures are estimated using deterministic models. TRANSYT-7F is a macroscopic deterministic optimization model which minimizes a performance index, defined as a weighted combination of system delay and stops. It models traffic in platoons using a platoon dispersion algorithm and considers queuing process by estimating arrival and discharging flow second by second. MAXBAND, PASSER II and TRANSYT-7F can all be considered as deterministic models because they only use average traffic volumes as optimization inputs. Traffic flow fluctuations are not considered in these models. As argued by Heydecker (1987), the degree of variability of traffic flows and signals has a significant impact on the outcome of signal optimization, in that using the average flows may incur considerable additional delay, compared with the timing obtained by taking this variability into account. In order to accommodate traffic variations, Synchro optimizes signal timing by averaging results of five volume scenarios (10, 30, 50, 70 and 90 percentiles), which assumes the user-input volumes are the means of random variables with Poisson distribution. However, these scenarios are arbitrarily assumed and they may not be consistent with actual traffic conditions in the field.

As indicated by Abbas et al. (2001), existing offset optimization models for vehicle-actuated coordinated traffic signals fails to address two important issues: (1) the early return to green problem because of the traffic flow variations on non-coordinated approaches, (2) the variation of waiting queue lengths at coordinated directions. Over the years, a number of research studies on offset optimization have attempted to address these two problems from different perspectives. To mitigate the “early-return-to-green” problem, Skabardonis (1996) developed several alternative procedures to modify controller yield points and phase force-offs using either the average spare green times or the average duration of the green times for the actuated phases. Shoup and Bullock (1999) developed an offline procedure to optimize offsets, assuming the availability of travel times between intersections from vehicle re-identification technologies. Abbas et al. (2001) developed a real-time offset transitioning algorithm for coordinated traffic signals. The algorithm uses a greedy approach to search for the optimal offset by moving the green window to include more vehicles that can pass during green time. Gettman et al. (2007) proposed a real-time control algorithm to adjust intersection offsets in a coordinated traffic signal system, based on the signal phase and detector data from the last several cycles. Using the archived signal status data, Yin et al. (2007) presented an offline offset refiner, which addresses the problem of uncertain green starts and ends in the determination of offsets. More recently, based on high resolution controller data, Day et al. (2010) introduced the Purdue Coordination

Diagram (PCD) to assess arterial coordination and Bullock et al. (2011) evaluated the performance of different offset optimization objective functions. However, none of the previous studies have addressed the two problems identified above simultaneously, which could lead to suboptimal solutions. These two problems are intertwined together, as traffic demand variations will lead to uncertain green start times, and uncertain green start times will result in stochastic length of waiting queues even with deterministic demands. The two problems, therefore, need to be considered simultaneously.

In this project, we propose a data-driven approach to optimize offsets for vehicle-actuated coordinated traffic signals, using the massive amount of signal status and vehicle actuation data collected from the field. The proposed model is intended to serve as an off-line offset fine-tuning tool, which optimizes the offsets after monitoring the traffic condition in the field for a certain period of time. The proposed approach, for the first time, addresses the two problems of vehicle-actuated traffic signal coordination simultaneously. To account for the early return to green problem, for the coordinated phase, we introduce the concept of conditional probability of the green start times, which can be obtained from the archived high-resolution traffic signal data. To handle the uncertainty of intersection queue length, we adopt a scenario-based optimization approach, which uses a series of traffic demand scenarios obtained from the archived data as the model input. The objective of this model is to minimize total delay for the main coordinated direction and at the same time considers the performance of the opposite direction. We test the performance of the optimized offsets not only in a simulated environment but also in the field. Results from both experiments show that the proposed model can reduce travel delay of coordinated direction without compromising the performance of the opposite direction. In practice, we envision that our optimization program can be utilized periodically (for example, every a few weeks) to optimize system performance using the archived data during that period.

The remainder of the report is organized as follows. In Chapter 2, we present the high-resolution traffic signal data and introduce two important concepts: the conditional distribution of green start times and the traffic demand scenarios. In Chapter 3, the scenario-based offset optimization model is presented. The solution method and optimization results are given in Chapter 4. The simulation and field tests are described in Chapter 5 and Chapter 6, respectively. Conclusions and further research directions are included in Chapter 7.

Chapter 2. High-Resolution Traffic Signal Data

The proposed offset optimization model is based on the traffic data collected by the SMART (Systematic Monitoring of Arterial Road Traffic)-Signal system (Liu and Ma, 2009, Liu, et al. 2009). The system is an integrated data collection, storage, and analysis system which can continuously collect and archive high resolution event-based traffic signal data including every vehicle-detector actuation and every signal phase change. Six intersections along the TH55 in Minneapolis, MN were chosen as the study site, as shown in Figure 2.1. This corridor has a total length of 1.83 miles with a speed limit of 55 MPH. The six intersections are operated in a vehicle-actuated coordinated mode during weekday's morning peak (7:00AM ~ 9:00 AM) and afternoon peak (3:30 PM ~ 5:30 PM), with a cycle length of 180 seconds. The coordination favors east bound (phase 2) traffic in the morning peak and west bound (phase 6) traffic in the afternoon. Ten weekdays' data during morning peak hours from 6/15/2009 to 6/26/2009 were used in this project.

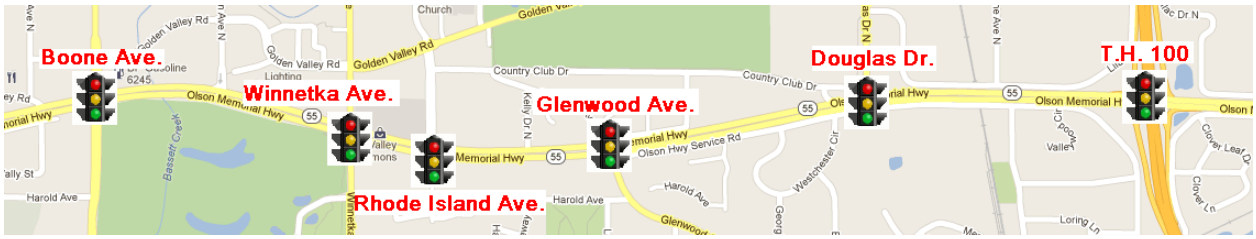

Figure 2.1: Installation of SMART-Signal system on TH55, Golden Valley, MN (Source: Google Maps).

2.1 Conditional Distribution of Green Start Times

As mentioned above, the SMART-Signal system archives every signal change and detector actuation at signalized intersections. Figure 2.2 presents an example distribution of green start times of the coordinated phase (Phase 2) in the local controller clock at the intersection of TH55 & Boone Ave. Figure 2.3 shows the corresponding dual-ring control diagram, which has 8 phases. Based on the settings, phase 2 and phase 6 are designated coordinated phases and a cycle starts at the time when phases 3 and 8 begin. Under different traffic conditions, the non-coordinated phases may be terminated due to gap-out or max-out, or at its force-off point. It can even be skipped if there is no vehicle actuation for a particular phase. Any unused green time from the non-coordinated phases would be added to the coordinated phases (i.e. phase 2 and phase 6), which makes the coordinated green start earlier, i.e. the so-called "early return to green" problem. In this case, the duration time of phase 3 and phase 4 would determine the green start time of phase 2, as can be seen from Figure 2.3. The minimum split length for phase 3 and phase 4 are 12 seconds and 16 seconds, respectively, and their maximum splits are 15 seconds and 26 seconds. One pedestrian phase is associated with phase 4, which has a "Walking" time of 7 seconds and a "Flashing Don't Walk" time of 30 seconds. Since the assigned pedestrian phase is longer than the duration of associated phase 4, if there is a pedestrian call, it will extend the phase 4 green beyond its original maximum. As a result, the green start time distribution in Figure 2.2 is clearly divided into three groups, as indicated by the red numbers. In group 1, either phase 3 or phase 4 is skipped, which makes phase 2 green start time smaller than the

summation of two minimum split lengths (12 + 16 = 28 seconds); In group 2, both phases are active in the cycle and the total spit length varies from its minimum to maximum (15 + 26 = 41 seconds); In part 3, there is at least one pedestrian call in the cycle which makes coordinated phase 2 starts later than usual.

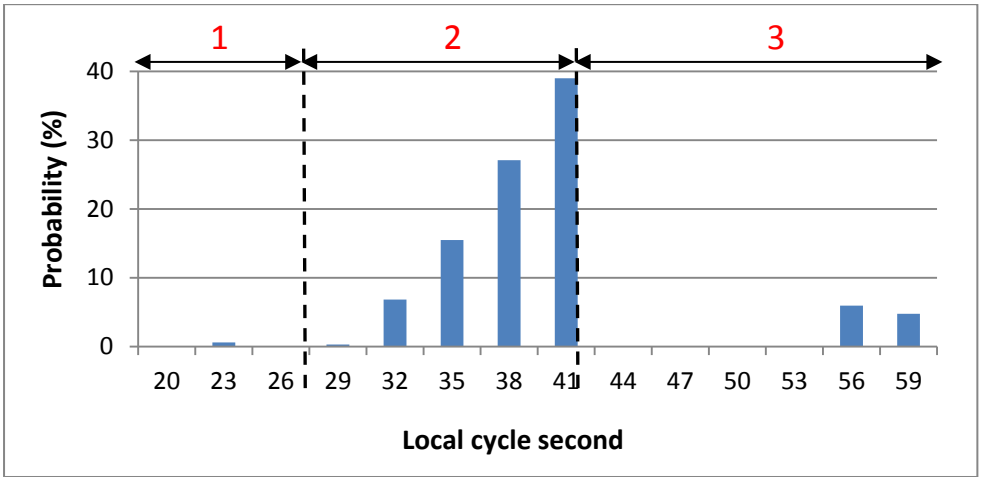

Figure 2.2: Distribution of green start time of Phase 2 (Coordinated phase) in local clock, TH 55 & Boone Ave, 7:00 AM ~ 9:00 AM, 6/15/2009 ~ 6/26/2009 10 weekdays.

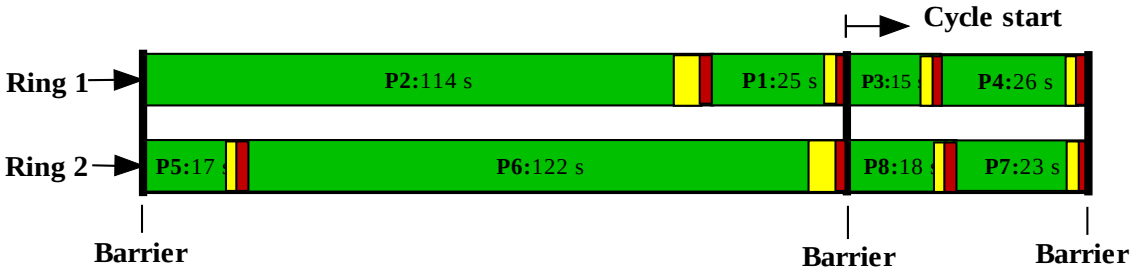

Figure 2.3: Dual-ring control diagram of intersection TH 55 & Boone Ave during weekday AM peaks.

As shown above, at vehicle-actuated intersections, signal timings vary from cycle to cycle under different actuation patterns and the "early return to green" problem of coordinated phases exist due to various reasons. The green start time of each coordinated phase is very much dependent on the vehicle actuations of non-coordinated phases. To represent this relationship, an associated number of vehicle actuations, $n_{i,p}$ for coordinated phase p of intersection i , is introduced.

Without loss of generality, a four-leg and 8-phase intersection is taken as an example. Intersection layout and corresponding dual-ring control diagram are shown in Figure 2.4. The numbers in the layout indicate different phases (phase 2 and phase 6 are coordinated phases here) and the red arrows indicate different moving directions. According to the dual ring control logic, different rings can only go across the "barriers" at the same time. Specifically, phase 3 and phase 8 should start at the same time and phase 4 and phase 7 should end at the same time. As a result, the non-coordinated phase in one ring with less vehicle actuations, which is supposed to end earlier, may be extended by the phases in the other ring with more vehicle actuations.

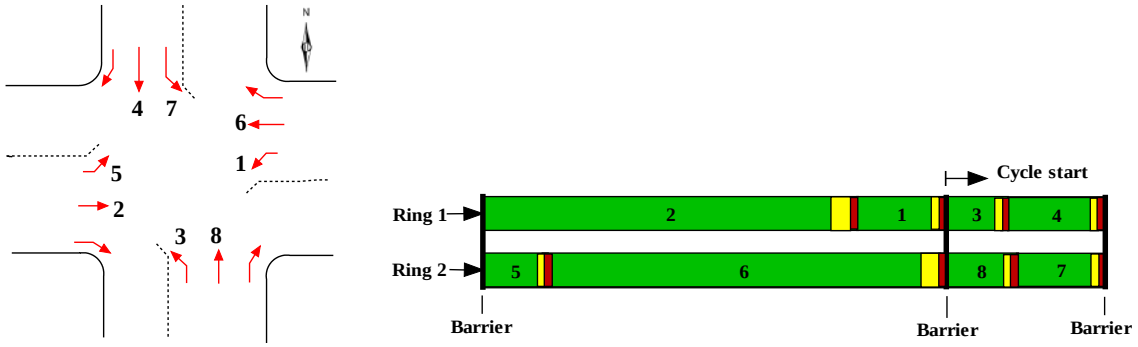

Figure 2.4: Dual Ring Control diagram of an example intersection.

Assume the number of actuations for a particular phase in each cycle is equal to the cycle input volume of that phase, which is usually the case for side streets because they have stop-bar detectors in place. The calculation of $n_{i,p}$ can be shown in Equation 2.1, where $N_{i,p}$ is the cycle input volume for phase p of intersection i. It states that the associated number of vehicle actuations of phase 2 is equal to the larger values between $N_{i,3}+N_{i,4}$ and $N_{i,7}+N_{i,8}$; for phase 6, the associated number of vehicle actuations is equal to the larger values between $N_{i,3}+N_{i,4}$ and $N_{i,7}+N_{i,8}$ plus the number of actuations of phase 5 ($N_{i,5}$). Note that phase 1 is not considered when calculating the associated number of vehicle actuations for phase 2, because the lagging phase after the coordinated phase usually has a fixed length of duration.

$$n_{i,2} = \max(N_{i,3}+N_{i,4}, N_{i,7}+N_{i,8})$$
$$n_{i,6} = \max(N_{i,3}+N_{i,4}, N_{i,7}+N_{i,8}) + N_{i,5} \qquad \text{Equation 2.1}$$

It is intuitive that the larger the $n_{i,p}$ is, the later the green phase of the coordinated phase p tends to start. Taking different arrival and actuation profiles of non-coordinated phases into consideration, the green start time of coordinated phase p can be different even if $n_{i,p}$ is the same. Therefore, for coordinated phase p, given its associated number of actuations $n_{i,p}$, we can get the distribution of green start time $G_{i,p}$. Note that, the introduction of the conditional distribution $P\left(G_{i,p} \mid n_{i,p}\right)$ is specifically designed to accommodate the "early return to green" problem for the coordinated phases. Even if the input volumes are the same, actual signal timings may still vary and the variation is consistent with field results, since all the distributions are derived from field data.

For example, Figure 2.5 categorizes the green start times of coordinated phase 2 at the intersection TH 55 & Boone Ave according to the associated number of actuations $n_{1,2}$. The data points are clearly divided into three groups, as discussed before. One can see that, within each group, as the associated number of actuations $n_{1,2}$ increases, the green start time of phase 2 tends to be later. Therefore, different values of associated number of vehicle actuations will lead to different distributions of green start time. The two plots in Figure 2.6 show the conditional

distributions when $n_{1,2}=6$ and $n_{1,2}=9$ respectively. We can see that there are two different distribution patterns. When $n_{1,2}=6$, the green start time are almost evenly distributed among 36, 39 and 42 seconds; however, when $n_{1,2}=9$, 60% of the time, phase 2 green would start at 42 seconds. Similarly, conditional distributions can be generated for phase 6 and also for other intersections.

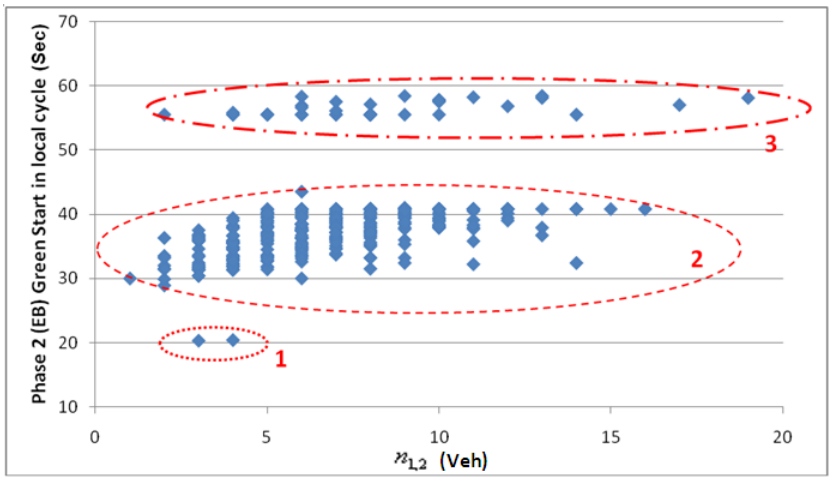

Figure 2.5: Phase 2 (Eastbound through) green start time vs. associated number of actuations, TH 55 & Boone Ave, 6/15/2009 ~ 6/26/2009 10 weekdays.

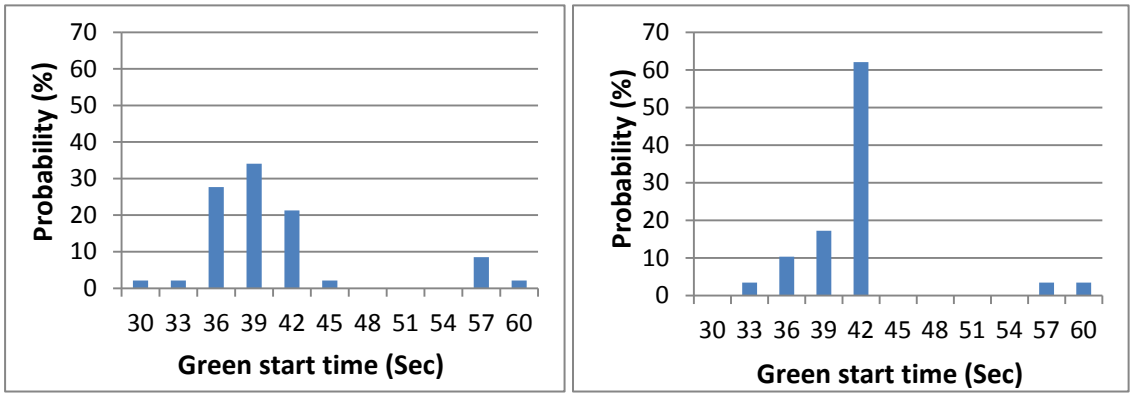

Figure 2.6: Conditional distributions of Phase 2 (EB) green start time $P(G_{1,2}\mid n_{1,2})$, (Left) $n_{1,2}$=6 (Right) $n_{1,2}$=9, TH 55 & Boone Ave, 6/15/2009 ~ 6/26/2009 10 weekdays.

2.2 Traffic Scenarios

Based on the high-resolution traffic signal data, traffic demands at the boundary of the arterial and turning percentages at each intersection can also be obtained. As shown in Figure 2.7, input volume of direction d at intersection i is denoted by $N_{i,d}$ ($i=1,2,...,I$, $d=$*Eastbound, Westbound, Northbound or Southbound*) and corresponding turning percentages are denoted by $\varphi_{i,d}^{x}$ ($x=$*Left, Right, Through*). Without loss of generality, we assume the arterial is coordinated

in the east-west direction. To deal with the uncertainty of traffic demand, a set of traffic scenarios $S = \{1, 2, ..., J\}$ is introduced. Each scenario $j \in S$ is a vector of boundary input volumes and turning percentages, i.e. $\left(N_{1,EB}^{(j)}, N_{1,SB}^{(j)}, ..., \varphi_{1,EB}^{L\,(j)}, \varphi_{1,EB}^{R\,(j)}, ...\right)^T$, with a probability of occurrence $p^{(j)}$. In general, the more scenarios we consider, the more robust the optimization results will be. But that will inevitably increase the complexity of the problem. According to Mulvey et al. (1995), a relatively small number of scenarios can still generate near-optimal results. In practice, the number of scenarios considered in the optimization model is constrained by the availability of dataset, available computational capability and etc, so users can choose the most suitable number of scenarios accordingly. In this project, 10 weekdays' morning peak (7:00 AM ~ 9:00 AM) data is utilized and every 15 minutes' interval is considered as one traffic scenario. In total, there are 80 scenarios. Within each scenario $j \in S$, the boundary input volumes $N_{i,d}^{(j)}$ and turning percentages $\varphi_{i,d}^{x\,(j)}$ are assumed to be stable and the values are set as the averages over all cycles within the 15-minute interval.

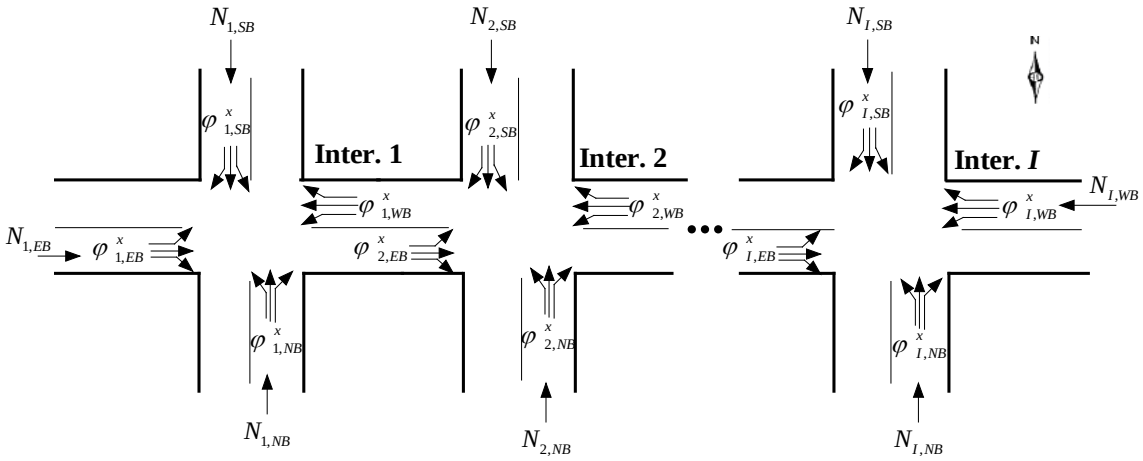

Figure 2.7: Boundary input volumes and turning percentages.

Given a scenario $j \in S$, the cycle input volumes for intermediate links can be calculated by Equation 2.2 and Equation 2.3. It is easy to find out that eastbound cycle input volume of intersection *i+1* is the summation of volumes of three movements at intersection *i* (eastbound through, southbound left and northbound right), as shown in Equation 2.2. Similarly, westbound cycle input volume of intersection *i-1* is calculated by Equation 2.3. By applying Equation 2.2 and Equation 2.3 to each intersection, the cycle volume of each movement becomes known.

$$N_{i+1,EB}^{(j)} = N_{i,EB}^{(j)} \times \varphi_{i,EB}^{T\,(j)} + N_{i,SB}^{(j)} \times \varphi_{i,SB}^{L\,(j)} + N_{i,NB}^{(j)} \times \varphi_{i,NB}^{R\,(j)} \qquad \text{Equation 2.2}$$

$$N_{i-1,WB}^{(j)} = N_{i,WB}^{(j)} \times \varphi_{i,WB}^{T\,(j)} + N_{i,SB}^{(j)} \times \varphi_{i,SB}^{R\,(j)} + N_{i,NB}^{(j)} \times \varphi_{i,NB}^{L\,(j)} \qquad \text{Equation 2.3}$$

Chapter 3. Model Formulation

3.1 Scenario-Based Offset Optimization

To account for the stochastic nature of field traffic, a data-driven optimization model is developed in this project to generate arterial offsets. As discussed in the previous section, based on the high-resolution traffic signal data, conditional distributions of green start time P and traffic scenarios S can be derived, which will be the model inputs in this project. In general, the optimization model can be represented by Equation 3.1, where the objective is to minimize the total travel delay D of coordinated directions. O is the vector of intersection offsets (decision variables) and Ω is the feasible set of O.

$$\min D(O,P,S) \quad s.t.\ O \in \Omega \qquad \text{Equation 3.1}$$

Given a traffic scenario $j \in S$, since the cycle volume for each movement can be calculated, the associated number of vehicle actuations, denoted by ${n_{i,p}}^{(j)}$, can be generated for the coordinated phases of each intersection. Then, given a feasible offset $O \in \Omega$, the expectation of travel delay for coordinated phase p under scenario j, denoted by $E\left({D_p}^{(j)}(O)\right)$, can be calculated by Equation 3.2. Note that, the conditional distribution of green start time for the coordinated phase at intersection i is assumed to be independent with that at intersection $i+1$. This assumption is reasonable because the green start time of coordinated phase at each intersection is determined by the corresponding vehicle actuations of non-coordinated phases and it is reasonable to assume they are independent.

$$E\left({D_p}^{(j)}(O)\right) = E\left(\sum_{i=1}^{I-1} {D_{i,p}}^{(j)}(O)\right) = \sum_{i=1}^{I-1} E\left({D_{i,p}}^{(j)}(O)\right)$$
$$= \sum_{i=1}^{I-1}\sum_{x}\sum_{y} D\left(o_i, o_{i+1}, x, y\right) P\left(G_{i,p} = x \mid n_{i,p} = {n_{i,p}}^{(j)}\right) P\left(G_{i+1,p} = y \mid n_{i+1,p} = {n_{i+1,p}}^{(j)}\right) \qquad \text{Equation 3.2}$$

Here O represents the offset vector $[o_1, o_2, ..., o_I]$ and $D(.)$ refers to the deterministic delay calculation model between two adjacent intersections given signal timings (i.e. offsets and green start times for coordinated phases) and traffic scenario, which will be introduced in the next section.

The best solution for arterial coordination would optimize the performance of two major directions at the same time. However, in most cases, the two directions cannot achieve optimality simultaneously and there is always a trade-off between the two. In this project, a weighting term $\alpha \in [0,1]$ is introduced to represent the importance of the minor coordinated direction and the weighted delay for both directions is calculated by Equation 3.3, where ${D_p}^{(j)}(O)$ and ${D_{p'}}^{(j)}(O)$ are the travel delays for major and minor coordinated directions respectively.

$$D^{(j)}(O) = (1-\alpha)E\left(D_p{}^{(j)}(O)\right) + \alpha E\left(D_{p'}{}^{(j)}(O)\right) \quad \text{Equation 3.3}$$

Given an intersection offset setting O, we can calculate the corresponding arterial delay series $D^{(1)}(O), D^{(2)}(O), ..., D^{(J)}(O)$ for different scenarios. Let $D_{(1)}(O), D_{(2)}(O), ..., D_{(J)}(O)$ be the descending order of the series, i.e., $D_{(1)}(O) \geq D_{(2)}(O) \geq, ..., \geq D_{(J)}(O)$. Obviously, the larger the value of D is, the worse the arterial performance will be. In practice, motorists and engineers may have different opinions about these scenarios and therefore a trimming factor $\beta \in [0,1]$ is introduced. The value of β represents the fraction of scenarios that will not be considered and the number of scenarios left after trimming is $J_\beta = \lfloor J(1-\beta) + \beta \rfloor$. If $\beta = 0$, there is no trimming ($J_\beta = J$) and all the scenarios are considered; However, if $\beta = 1$, $J_\beta = 1$, only the worst scenario $D_{(1)}(O)$ will be considered. Therefore, the measure of arterial delay given intersection offset setting O can be formulated as $\frac{1}{J_\beta}\sum_{k=1}^{J_\beta} D_{(k)}(O)$ and $D_{(k)}(O)$ is the k-th largest delay value. The general form of the scenario-based offset optimization model is shown in Equation 3.4 and the deterministic delay calculation model will be introduced in the next section. Note that, under transformed time coordinates (i.e. shifted according to the free flow travel time from the first intersection), intersection offsets vary from $-c/2$ to $c/2$, where c is the common cycle length.

$$\begin{aligned} &\min \frac{1}{J_\beta}\sum_{k=1}^{J_\beta} D_{(k)}(O) \\ &s.t.\ O \in \Omega, \\ &\Omega = \left\{ [o_1, o_2, ..., o_I] : -\frac{c}{2} \leq o_i \leq \frac{c}{2}, \forall i \right\} \end{aligned} \quad \text{Equation 3.4}$$

3.2 Delay Calculation

In this project, the delays caused by main street and side street traffic are specifically considered in the delay calculation model, as will be described in this section. Given intersection signal timings (i.e. offsets and green start times for coordinated phases) and traffic scenario (i.e. traffic demand for each approach), the calculation of delays for coordinated directions becomes a deterministic problem. Since the red time durations of coordinated phases have direct association with the calculation of travel delay for coordinated directions, green start times $G_{i,p}$ are first converted into red time durations $r_{i,p}$ .in the delay calculation model.

The calculation for one coordinated direction is first considered since the calculation for the opposite direction can follow the same way. In the following, we take the eastbound (a coordinated direction) as an example and for simplicity purpose the subscript *p* is omitted. At each intersection *i*, cycle input volumes to the downstream intersection can be separated into two parts. One is discharged from side streets when coordinated phase is red, denoted by W_i^s ; the

other is discharged from main street when coordinated phase is green, denoted by W_i^m. For example, for eastbound traffic, W_i^s is equal to $N_{i,SB} \times \varphi_{i,SB}^L + N_{i,NB} \times \varphi_{i,NB}^R$ and W_i^m is equal to $N_{i,EB} \times \varphi_{i,EB}^T$. Assume vehicles are uniformly arrived during red and green period of the coordinated phase and they are evenly distributed at downstream lanes, the arrival flow rate per lane to downstream intersection in these two periods can be calculated by Equation 3.5, where q_i^s and q_i^m (veh/sec/lane) are the arrival flow rate per lane to downstream intersection formed by side street traffic (during the red time of the coordinated phase) and main street traffic (during the green time of the coordinated phase) respectively, and z_i is number of lanes at downstream link.

$$q_i^s = W_i^s / r_i / z_i$$
$$q_i^m = W_i^m / (c - r_i) / z_i$$

Equation 3.5

In the delay calculation model, time coordinate of each intersection is shifted according to the free flow travel time from the first intersection. Vehicle trajectory then becomes a vertical line in the time-space diagram if there is no stop or delay (see Figure 3.1 and Figure 3.2). Assume the offset reference point is the green end (or red start) of corresponding coordinated phase. Two variables d_i^c and d_i^g are introduced to represent the time difference of cycle starts and green starts between intersection i and downstream intersection $i+1$ under the transformed time coordinates. The definition is shown in Equation 3.6, where o_i is the offset value and r_i is the red duration time of coordinated phase at intersection i. Based on the sign of d_i^c, the delay calculation process is divided into two cases.

$$d_i^c = o_{i+1} - o_i$$
$$d_i^g = o_{i+1} + r_{i+1} - o_i - r_i$$

Equation 3.6

1) $d_i^c \geq 0$

In this case the upstream red light for the coordinated phase starts earlier than that of the downstream intersection (See Figure 3.1). Depending on the start time of the downstream green light, vehicles discharged from upstream side streets with an arrival rate q_i^s may cause a queue at the downstream intersection; After the upstream intersection turns green, downstream intersection will have arrival vehicles from upstream coordinated phase with a rate of q_i^m. Under different values of d_i^g and arrival flows, this portion of vehicles may or may not cause a queue at downstream. For example, if $d_i^g \geq 0$, as shown in Figure 3.1, upstream green starts earlier than downstream and part of the upstream main street flow will definitely cause a queue at downstream; if $d_i^g < 0$, downstream green starts earlier than upstream, so the queue may be cleared before the arrival of upstream main street vehicles. If t_i^q is used to represent the portion of green at intersection *i* within which discharged vehicles will cause a queue at downstream and

q_{i+1}^d (Veh/sec) is the discharging rate of intersection $i+1$, the following flow conservation equation holds.

$$(r_i - d_i^c)q_i^s + t_i^q q_i^m = (t_i^q - d_i^g)q_{i+1}^d \qquad \text{Equation 3.7}$$

t_i^q can be calculated by solving Equation 3.7. $t_i^q = 0$ when upstream main street flow does not cause a queue at downstream. Since t_i^q cannot be negative,

$$t_i^q = \max\left\{\frac{(r_i - d_i^c)q_i^s + d_i^g q_{i+1}^d}{q_{i+1}^d - q_i^m}, 0\right\} \qquad \text{Equation 3.8}$$

The first vehicle from coordinated phase of intersection i which has no delay at downstream will have the trajectory of CC' in Figure 3.1. Note that h represents the jammed space headway in the figure. The area of the shadowed triangle ΔDEF divided by h represents the total delay (Veh.Sec) of all the vehicles discharged from coordinated phase of intersection i in one cycle. The delay D_i can be calculated by Equation 3.9. Note that the area of the triangle may be zero if the upstream main street traffic does not cause a queue at downstream.

$$D_i = Ar(\Delta DEF)/h = \frac{|DE| \times |FG|}{2h} = \frac{\left\{d_i^g + \frac{(r_i - d_i^c)q_i^s}{q_{i+1}^d}\right\} \times (q_i^m t_i^q)}{2} \qquad \text{Equation 3.9}$$

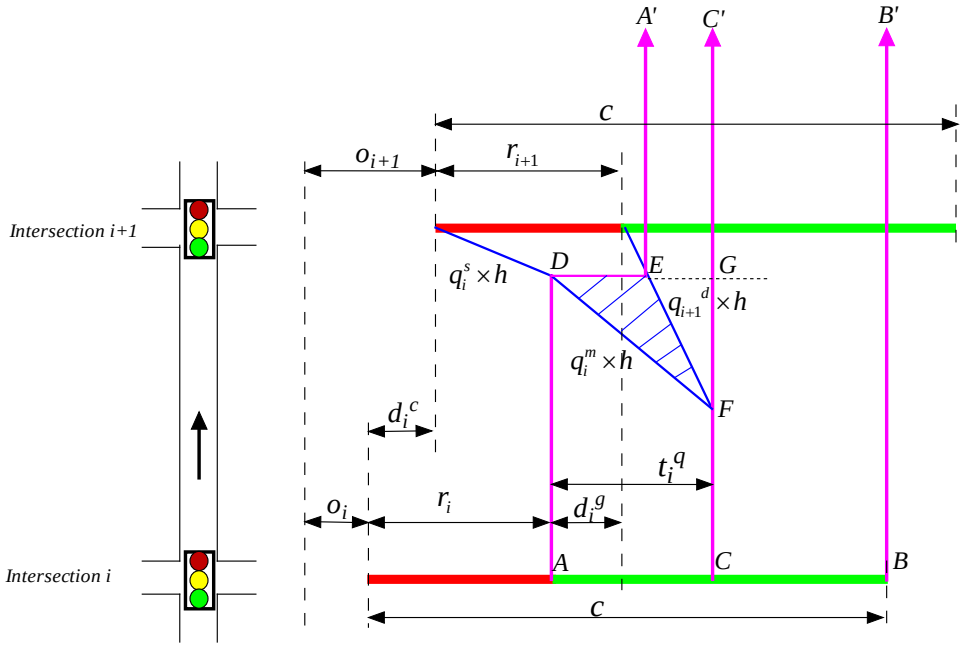

Figure 3.1: Queuing process between two intersections when $d_i^c \geq 0, d_i^g \geq 0$.

2) $d_i^c < 0$

In this case, upstream red of the coordinated phase starts later than the downstream intersection. Vehicles discharged at the end of green of upstream intersection will cause a residual queue at downstream and the queuing curve is shown as HJ in Figure 3.2. After upstream coordinated phase turns red, vehicles from upstream side streets will keep increasing the downstream queue with an arrival rate of q_i^s. After upstream coordinated phase turns green, downstream intersection will have arrival vehicles from upstream coordinated phase with a rate of q_i^m (Veh/sec). If $d_i^g \geq 0$, as shown in Figure 3.2, upstream main street flow will cause a queue at downstream; if $d_i^g < 0$, upstream main street vehicles may or may not cause a queue at downstream depending on the arrival flow rate. According to flow conservation, Equation 3.10 holds.

$$-d_i^c q_i^m + r_i q_i^s + t_i^q q_i^m = (t_i^q - d_i^g) q_{i+1}^d \qquad \text{Equation 3.10}$$

t_i^q can be derived from Equation 3.10 and $t_i^q = 0$ when upstream main street flow does not cause a queue at downstream. Therefore, t_i^q can be represented by

$$t_i^q = \max\left\{\frac{-d_i^c q_i^m + r_i q_i^s + d_i^g q_{i+1}^d}{q_{i+1}^d - q_i^m}, 0\right\} \qquad \text{Equation 3.11}$$

The total delay of the main street traffic includes two parts, trapezium $HIKJ$ and triangle DEF, as shown in the shadowed area in Figure 3.2. $HIKJ$ represents the delay caused by residual vehicles discharged at the end of green of upstream coordinated phase and DEF is the delay caused by new arrival main street traffic. Note that the area of DEF could be zero if downstream queue is cleared before upstream main street vehicles arrive.

$$D_i = Ar(HIKJ)/h + Ar(DEF)/h$$

$$= \frac{[r_{i+1} + (r_i + d_i^g)] \times [-d_i^c q_i^m] + [-d_i^c q_i^m]^2 / q_{i+1}^d}{2} + \frac{\left\{d_i^g + \frac{r_i q_i^s + (-d_i^c q_i^m)}{q_{i+1}^d}\right\} \times (t_i^q q_i^m)}{2} \qquad \text{Equation 3.12}$$

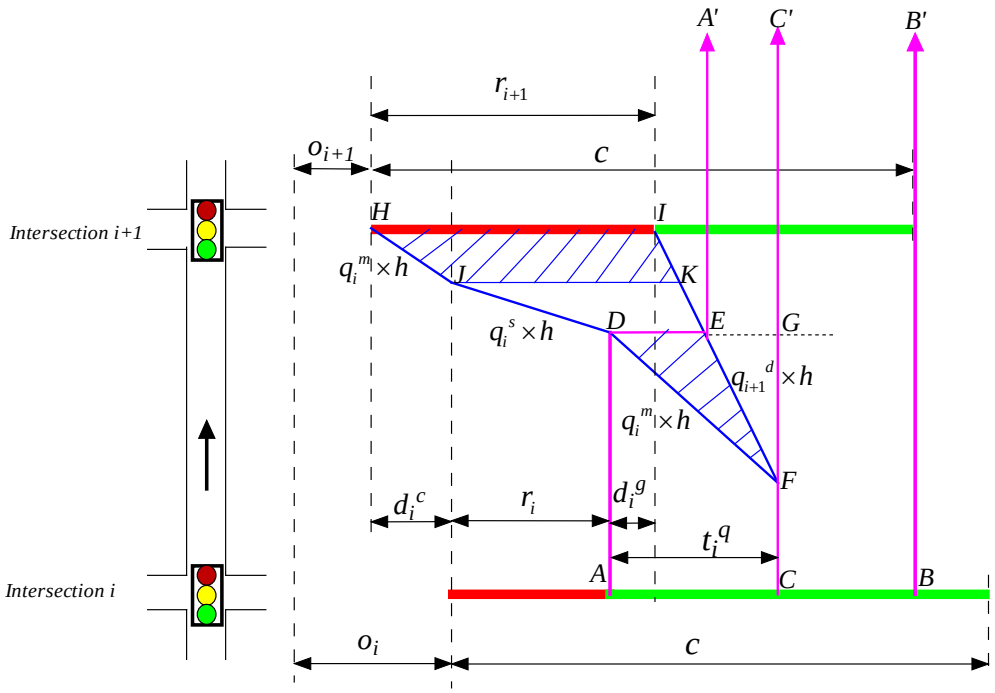

Figure 3.2: Queuing process between two intersections when $d_i^c < 0, d_i^g \geq 0$.

Based on the analysis above, the travel delay for coordinated phases between each two adjacent intersections can be calculated accordingly given intersection signal timings and traffic scenario. Therefore, the scenario-based offset optimization model is complete by taking the deterministic delay calculation model into Equation 3.4.

Chapter 4. Solution Method and Optimization Results

Since the feasible region of intersection offsets, i.e. Ω, is a closed convex set (see Equation 3.4) and the objective function is continuous and bounded within this region, an optimal solution to the problem must exist. Due to the complexity of the objective function, Genetic Algorithm (GA) is adopted to solve the problem. GA is a solution algorithm which mimics natural selection process. First, a population of solutions (chromosomes) is generated according to a creation rule, typically, in a random fashion. And then, the algorithm modifies the population of individual solutions repeatedly. At each step, depending on chromosome fitness, the algorithm selects chromosomes at random from the current population to be parents and every two parent chromosomes will produce two new offspring chromosomes based on a cross-over rule. The process repeats itself until certain stopping criteria is met, at which time the best solution remains in the population become the final solution O^*.

In this project, 10 weekdays' (6/15/2009 ~ 6/26/2009) morning peak (7:00AM ~ 9:00 AM) data of 6 intersections along the TH55 were chosen to generate the optimal offsets. In the GA solving process, since we can take the first intersection as the master intersection with an offset of 0, each chromosome would have the length of 5, where each gene indicates the offset value of corresponding intersection. For the sake of simplicity, we take $\beta = 0$, which means there is no trimming ($J_\beta = J$) and we consider all traffic scenarios. The weighting term α is assigned a value 0.1, meaning that 10 percent of weight has been assigned to the performance of minor direction in our objective function. Using a GA toolbox in Matlab with following parameters shown in Table 4.1, a solution can be achieved after about 30 generations for the offset optimization of the six intersections on TH55.

Table 4.1: Parameters for GA.

Population Size	Scaling Function	Elite Count	Crossover Fraction	Crossover Function	Mutation Function	Mutation Rate
400	Rank	2	0.8	Two point	Uniform	0.1

Figure 4.1 shows the GA results at each generation, where the star "*" shows the mean function value among all individuals at corresponding generation and "." represents the function value of the best-fitted individual. Finally, the program generates the offset result {0, -21.4, -21, -20.9, -21.1, -21.2} for six intersections from Boone Ave. to TH100 respectively, comparing with the field offset setting {0, -24.9, -21.6, 4.6, -20.5, -11.9} under the transformed time coordinates. The final optimized offset values applied to controllers are {0, 8, 25, 47, 79, 114} and this offset setting generates a weighted total cycle delay of 304 (Veh.Sec), comparing with 638 (Veh.Sec) under the field offset setting.

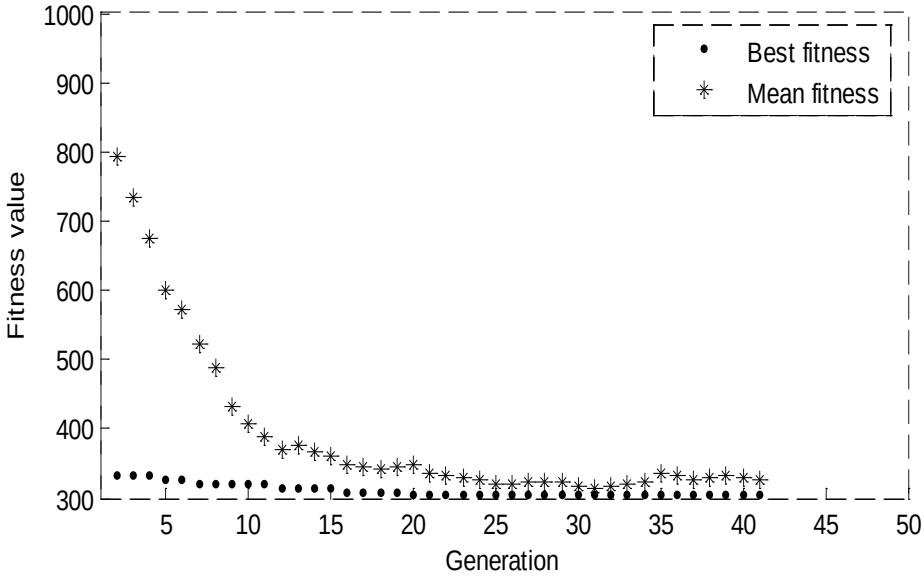

Figure 4.1: GA results for each generation.

Figure 4.2 shows the coordination result for both field and optimized offset setting in the time-space diagram under the transformed time coordinates. The two figures on the left hand side show the field coordination for both phase 2 and phase 6 and the two on the right show the optimized result. The arrows show the traffic direction for corresponding phases. Since original field offsets were already optimized by Synchro (the metropolitan district of Minnesota Department of Transportation retimes its traffic signals on all major arterials every 36 months or less), the generated offset values are very similar with the field ones. Major changes happen to Glenwood (4^{th} intersection) and TH100 (6^{th} intersection) with a 25.5 and 9.3 seconds' reduction respectively. It is hard to directly tell the difference from the coordination figure, but as we will demonstrate in the next section, the optimized offset will further improve the performance of the coordinated phase (eastbound of TH55) and without deterioration of the performance of the opposite direction (westbound of TH55).

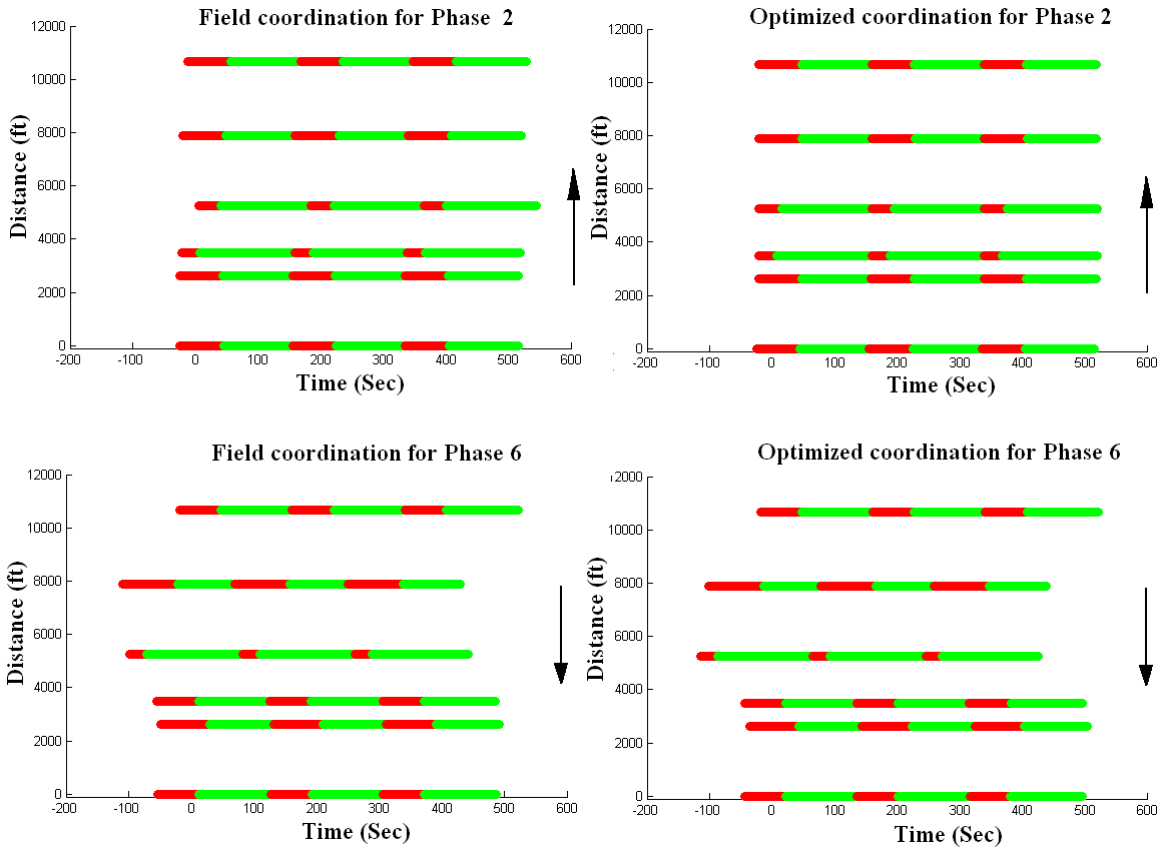

Figure 4.2: Coordination result for both field and optimized offsets.

Chapter 5. Evaluation Using a Simulation Model

In order to verify the performance of the offset results generated by the proposed model, a test network was built in VISSIM, as shown in Figure 5.1. Different traffic scenarios generated from the field data set were coded in the network, and signal controller's parameters, such as minimum green, maximum green and vehicle extension, were all configured according to the field settings. The simulation model was well calibrated in order to reveal the real traffic condition in the field. Figure 5.2 compares the distribution of coordinated green start time between simulation and field. The red columns represent the real distribution from the field while the blue columns show the simulation results. As one can see, simulation results match with field results very well at each intersection.

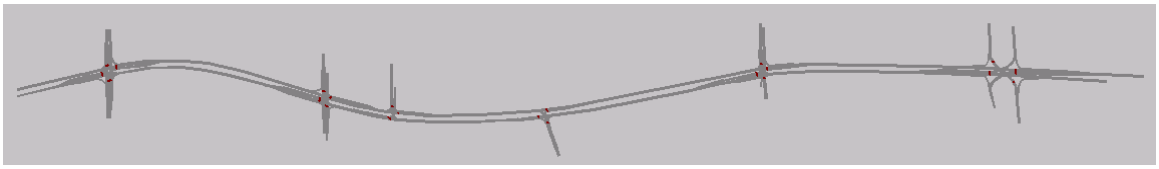

Figure 5.1: VISSIM network for test corridor.

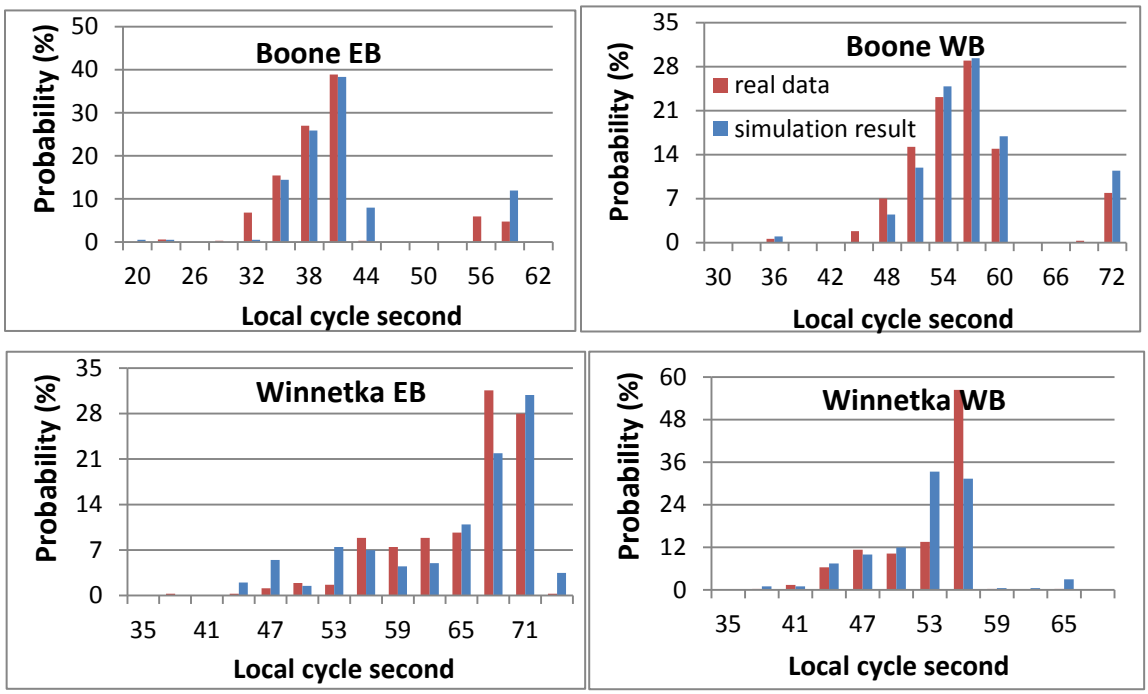

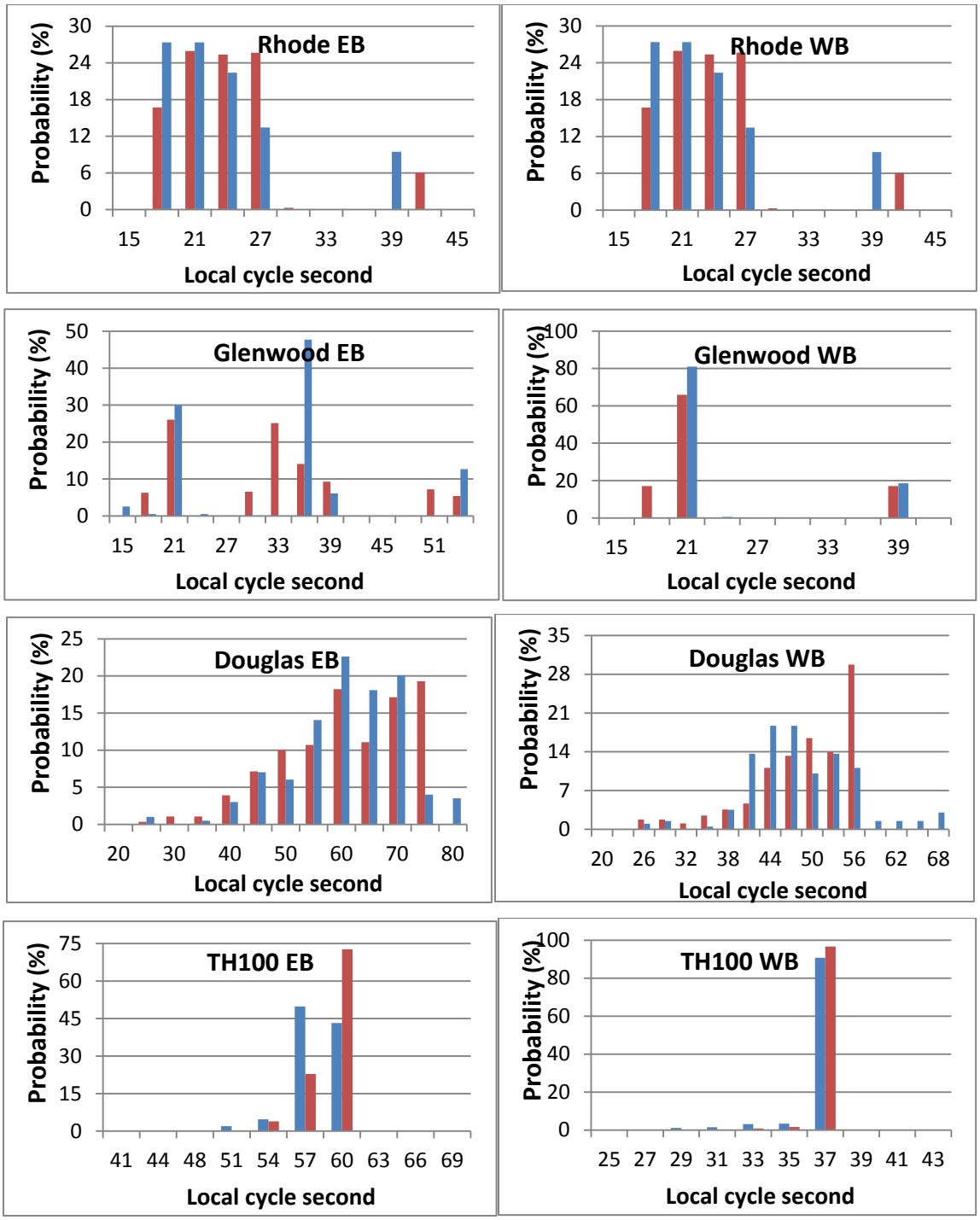

Figure 5.2: Comparison of distribution of coordinated green start between simulation model and the field.

The simulation was run for 20 times using 20 different random seeds. In order to compare the performance, both the offset setting in the field and the one generated by the optimization model were tested in the VISSIM network and we output the average delay of vehicles traversing both eastbound and westbound. The result is shown in Figure 5.3 and Table 5.1. As we can see, the

optimized offset result did improve the performance of east bound traffic, i.e. reduce travel delay by 13.9% on average. And at the same time, it did not make the westbound traffic worse.

In order to test the statistic significance of this improvement of eastbound, a paired t-test has been done to the two sets of travel times, i.e. under original offsets and under optimized offsets. The null hypothesis is that the two data sets come from distributions with the equal means. It turns out that we can reject the hypothesis with a *p* value 7.5649E-17 at the 5% significance level, which means the travel delay improvement is significant.

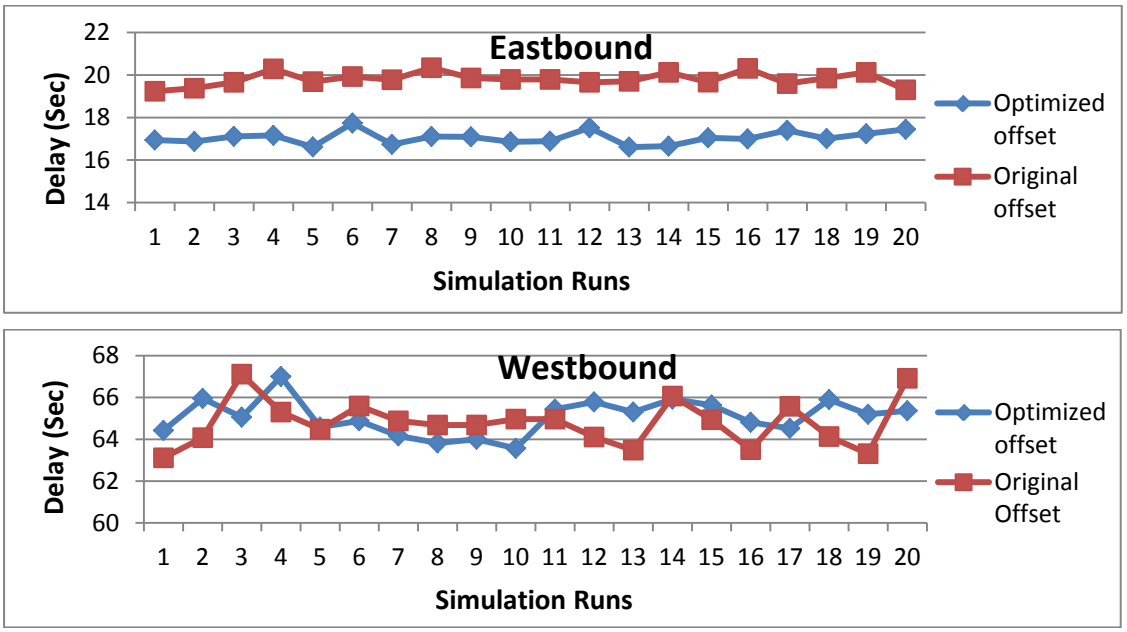

Figure 5.3: Simulation result of travel delay based on different offset settings.

Table 5.1: Eastbound and Westbound average delay comparison.

	Original Offset	Optimized Offset	Change
Eastbound Average Delay (Sec)	19.80	17.05	-13.90%
Westbound Average Delay (Sec)	64.80	65.06	0.42%

Chapter 6. Field Evaluation

The optimized offset values were implemented to the 6 intersections in the field for morning peak hours (7:00AM~9:00AM) on 9/14/2009. In order to compare the performance measures before and after the field implementation, two days with similar volume inputs need to be chosen. After examining 10 days before and after, 9/3/2009 was selected as the baseline day with original offset setting to compare with 9/14/2009. Table 6.1 shows the comparison of Eastbound and Westbound (major direction) input volume during two hours' peak period and Table 6.2 shows the comparison for side street input volumes. As we can see, the two major directions' input volumes for the two days are very similar and the day with optimized offset (9/14/2009) carries a little higher traffic. For side streets, these differences of input volumes are also within acceptable ranges.

Table 6.1: Eastbound and Westbound input volume (7:00AM~9:00AM) comparison between 9/3/2009 and 9/14/2009.

	9/3/2009 (Original offset)	9/14/2009 (Optimized offset)	Change Percentage
Eastbound Input Volume	4615	4647	0.69%
Westbound Input Volume	1817	1881	3.52%

Table 6.2: Side street input volume (7:00AM~9:00AM) comparison between 9/3/2009 and 9/14/2009.

		9/3/2009 (Original offset)	9/14/2009 (Optimized offset)	Change Percentage
Boone	Southbound	531	551	3.77%
	Northbound	445	452	1.57%
Winnetka	Southbound	748	675	-9.76%
	Northbound	285	269	-5.61%
Rhode	Southbound	456	470	3.07%
	Northbound	-*	-	-
Glenwood	Southbound	-	-	-
	Northbound	227	256	12.78%
Douglas	Southbound	943	934	-0.95%
	Northbound	213	207	-2.82%
TH 100	Southbound	586	622	6.14%
	Northbound	1008	923	-8.43%

*: T intersection, not applicable

Based on the high resolution data collected by the SMART-Signal system , intersection queue length for each cycle at each of the intersections were estimated using the algorithm developed by Liu, et al. (2009). In order to compare the performance of the 6-intersection corridor before and after the implementation of the optimized offsets, arterial travel times for both directions were also calculated as part of the SMART-Signal system based on the virtual probe algorithm developed by Liu and Ma (2009). Note the queue length estimation algorithm and the arterial travel time estimation algorithms implemented as part of the SMART-Signal system has been tested and evaluated in the past and it is currently in operation on a number of intersections in Minnesota and California (for more information on the SMART-Signal implementation, please see http:// dotapp4.dot.state.mn.us/smartsignal). Since we only have 6 intersections, performance in between is what we are interested in. Therefore, travel time between stop line of Boone and stop line of TH100 is taken as an indicator of corridor performance.

Table 6.3 compares the calculated travel delays of both eastbound (from stop line of Boone to stop line of TH100) and westbound (from stop line of TH100 to stop line of Boone) based on different offset settings. As we can see, both eastbound and westbound travel delays are substantially reduced after the offset adjustment. On average, the eastbound travel delay with original offset (9/3/2009) is 11.98 seconds and it decreases to 10.14 seconds after optimization (9/14/2009), which is a 15.3% reduction. For westbound, average travel delay with original offset is 78.48 seconds and it decreases to 70.84 seconds after optimization, which indicates a 9.7% reduction. Considering that the original offset setting was already optimized, the improvement is significant. One may notice that the absolute values of eastbound and westbound average delays are different with the values from simulation as listed in Table 5.1, because the actual demand and actuation profiles in the field cannot be the same with the ones in simulation. Figure 6.1 also compares the estimated eastbound queue length profiles during the one hour period at intersections 4 and 6 (where the major changes to offset happen) under different offset settings. One can find out that, in general, the optimized offset generates shorter queue lengths than the original offset. Therefore, the optimized offset outperforms the original offset not only in simulation but also in realistic field implementation.

Table 6.3: Eastbound and Westbound average delay comparison between 9/3/2009 and 9/14/2009.

	9/3/2009 (Original)	9/14/2009 (Optimized)	Change Percentage
Eastbound Average Delay (Sec)	11.98	10.14	-15.3%
Westbound Average Delay (Sec)	78.48	70.84	-9.7%

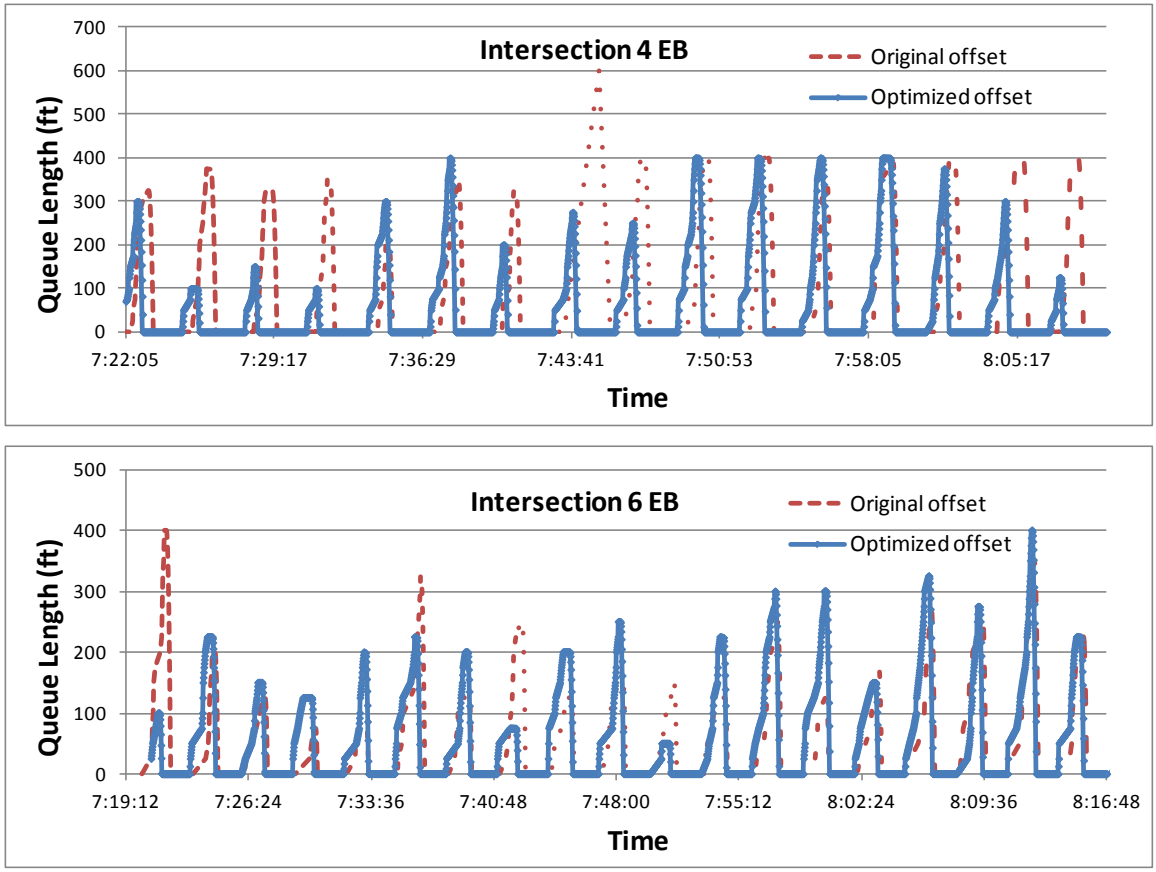

Figure 6.1: Estimated EB queue length based on different offset settings.

Chapter 7. Conclusions and Future Research

In this project, we propose an innovative approach for arterial offset optimization based on the large amount of high-resolution field traffic data. The model solves the two well-known problems with actuated signals: (1) the early return to green problem for coordinated phases and (2) the uncertainty problem of queue sizes formed at intersections. To account for the two problems, we introduce the concepts of conditional distribution of the green start times and traffic demand scenarios, both of which can be obtained from the high-resolution traffic dataset. We explicitly consider the queues formed by side-street and main-street traffic under different situations. The objective of this model is to minimize total delay for one coordinated direction and at the same time take the performance of the other direction into consideration. Because of the complexity of the objective function, the problem is solved by the Genetic Algorithm. We implemented our optimized offset values to both VISSIM simulation model and the field signal controllers. Both test results indicate that the model successfully optimizes the offsets along the signalized arterials. It improves the performance of the corridor significantly.

Looking forward, we envision that our optimization program can be utilized periodically (for example, every a few weeks) to optimize system performance using the archived data during that period. In the state-of-the-art practice, for most of the traffic management agencies, signal retiming is only conducted once every 3 to 5 years because it involves largely manual processes. But it is commonly understood that traffic delay increases 3-5% per year simply due to the fact that the timing plans are not kept up to date. For many resource-limited agencies, it would be desirable to replace the labor-intensive signal re-timing process with algorithms for automated or semi-automated updating of the signal parameter settings. The availability of the massive amount of high-resolution traffic signal data has made this possible. Although our offset optimization is moving one step further along this direction, it should be extended to include other signal control parameters such as green splits. We leave these topics for future studies.

References

[1] M. Abbas, D. Bullock, and L. Head, "Real-time offset transitioning algorithm for coordinating traffic signals," *Transportation Research Record,* Vol.1748, pp.26–39, 2001.

[2] D. Bullock, C. Day, Jr, T. Brennan, A. Hainen, S. Remias, H. Premachandra, J. Sturdevant, G. Richards, and J. Wasson, "Reliability, flexibility and environmental impact of alternative arterial offset optimization objective functions," *Proceedings of Transportation Research Board Annual Meeting,* Washington, DC. 2011.

[3] C. Day, R. Haseman, H. Premachandra, , T. Brennan, J. Wasson, J. Sturdevant, and D. Bullock, "Evaluation of arterial signal coordination. Methodologies for visualizing high-resolution event data and measuring travel time," *Transportation Research Record,* Vol.2192, pp.37–49. 2010.

[4] D. Gettman, S. Shelby, L. Head, and D. Bullock. "Data-driven algorithms for real-time adaptive tuning of offsets in coordinated traffic signal systems," *Transportation Research Record,* Vol.2035, pp.1-9. 2007.

[5] B. Heydecker. "Uncertainty and variability in traffic signal calculations," *Transportation Research Part B,* Vol.21 No.1, pp.79-85. 1987.

[6] H. Liu, X. Wu, W. Ma, and H. Hu. "Real-Time Queue Length Estimation for Congested Signalized Intersection," *Transportation Research Part C,* Vol.17 No.4, pp.412-427. 2009.

[7] H. Liu, and W. Ma. "A Virtual Vehicle Probe model for Time-dependent travel time Estimation on Signalized Arterials," *Transportation Research Part C,* Vol.17 No.1, pp.11-26. 2009.

[8] J. Little, M. Kelson, and N. Gartner. "MAXBAND: A Versatile program for Setting Signals on Arteries and Triangular Networks," Working paper 1185-81. Sloan School of Management, Massachusetts Institute of Technology. 1981.

[9] C.J. Messer, H.E. Haenel, and E.A. Koeppe. *Report on the User's manual for Progression Analysis and Signal System Evaluation Routine – PASSER II*. Texas Transportation Institute Report 165-14, Texas A&M University. 1974.

[10] J.M. Mulvey, R.J. Vanderbei, and S.A. Zenios. "Robust optimization of large-scale systems," *Operations Research,* Vol43 No.2, pp.264-281. 1995.

[11] A. Skabardonis. "Determination of timings in signal systems with traffic-actuated controllers," *Transportation Research Record,* Vol.1554, pp.18-26. 1996.

[12] G. Shoup, and D. Bullock. "Dynamic offset Tuning Procedure using travel time data," *Transportation Research Record,* Vol.1683, pp.84-94. 1999.

[13] Texas Transportation Institute. *PASSER V Guide*, http://ttisoftware.tamu.edu/docs/PASSER_V-09_Guide.pdf , 2009.

[14] C.E. Wallace, K.G. Courage, D.P. Reaves, G.W. Schoene, and G.W. Euler. *TRANSYT-7F User's Manual*. Transportation Research Center, University of Florida, Report No. UF-TRC-U32 FP-06/07, 1984.

[15] Trafficware. *Synchro 5.0 User's Guide*. Albany, California, 2001.

[16] Y. Yin, M. Li, and A. Skabardonis. "Offline Offset Refiner for Coordinated Actuated Signal Control Systems," *ASCE Journal of Transportation Engineering*, Vol.133 No.7, pp.423-432. 2007.